www.nature.com/aps

Acta Pharmacologica Sinica

ARTICLE

Aristolochic acid I promoted clonal expansion but did not induce hepatocellular carcinoma in adult rats

Yong-zhen Liu[1,2], Heng-lei Lu[1,2], Xin-ming Qi[2], Guo-zhen Xing[2], Xin Wang[2], Pan Yu[2], Lu Liu[2], Fang-fang Yang[2], Xiao-lan Ding[2], Ze-an Zhang[1], Zhong-ping Deng[1], Li-kun Gong[2,3] and Jin Ren[2]

Aristolochic acid I (AAI) is a well-known nephrotoxic carcinogen, which is currently reported to be also associated with hepatocellular carcinoma (HCC). Whether AAI is a direct hepatocarcinogen remains controversial. In this study we investigated the association between AAI exposure and HCC in adult rats using a sensitive rat liver bioassay with several cofactors. Formation of glutathione S-transferase placental form-positive (GST-P$^+$) foci was used as the marker for preneoplastic lesions/clonal expansion. We first conducted a medium-term (8 weeks) study to investigate whether AAI had any tumor-initiating or -promoting activity. Then a long-term (52 weeks) study was conducted to determine whether AAI can directly induce HCC. We showed that oral administration of single dose of AAI (20, 50, or 100 mg/kg) in combination with partial hepatectomy (PH) to stimulate liver proliferation did not induce typical GST-P$^+$ foci in liver. In the 8-week study, only high dose of AAI (10 mg · kg^{-1} · d^{-1}, 5 days a week for 6 weeks) in combination with PH significantly increased the number and area of GST-P$^+$ foci initiated by diethylnitrosamine (DEN) in liver. Similarly, only high dose of AAI (10 mg· kg^{-1}· d^{-1}, 5 days a week for 52 weeks) in combination with PH significantly increased the number and area of hepatic GST-P$^+$ foci in the 52-week study. No any nodules or HCC were observed in liver of any AAI-treated groups. In contrast, long-term administration of AAI (0.1, 1, 10 mg· kg^{-1}· d^{-1}) time- and dose-dependently caused death due to the occurrence of cancers in the forestomach, intestine, and/or kidney. Besides, AAI-DNA adducts accumulated in the forestomach, kidney, and liver in a time- and dose-dependent manner. Taken together, AAI promotes clonal expansion only in the high-dose group but did not induce any nodules or HCC in liver of adult rats till their deaths caused by cancers developed in the forestomach, intestine, and/or kidney. Findings from our animal studies will pave the way for further large-scale epidemiological investigation of the associations between AA and HCC.

Keywords: aristolochic acid I; glutathione S-transferase placental form-positive foci; clonal expansion; hepatocellular carcinoma; medium-term rat liver bioassay; DNA adducts

Acta Pharmacologica Sinica (2021) 42:2094–2105; https://doi.org/10.1038/s41401-021-00622-7

INTRODUCTION

Aristolochic acids (AA) are a family of nitrophenanthrene carboxylic acids found in plants from the *Aristolochiaceae* family, primarily of the genera Aristolochia and Asarum. Botanical products derived from plants containing AA have been used in traditional folk remedies for thousands of years. AA has a wide range of pharmacological effects, including antibacterial, anti-inflammatory, analgesic, and antitumor effects. It is commonly used in the treatment of eczema, pneumonia, and stroke [1]. However, its use is limited/banned due to its toxicity in the liver, kidney, and gastrointestinal tract and its carcinogenicity found in recent years [2–11]. AA has been found to be the etiologic agent of endemic nephropathy in the Balkan region and contributes to chronic kidney disease and upper urinary tract urothelial cell carcinoma (UCC) [12–22].

Currently, a few herbs containing trace amounts of AA are still allowed on the market. In China, the government and various research institutes have reevaluated the usage and circulation of AA-containing herbs and have updated regulations and solutions accordingly. Only three botanical products derived from plants of the Aristolochia family, namely, Aristolochia/Madouling, Aristolochiae Herba/Tianxian Teng, and *Asarum heterotropoides*/Xixin, are included in the Chinese Phsarmacopoeia (Ch. P) 2015 Edition [23, 24]. Aristolochia, which has a relatively low AA content, is commonly used for the treatment of lung complaints including asthma, although its maximal recommended human daily dose (MRHD) is limited to 9 g, and the maximum content of aristolochic acid I (AAI) was not defined. It has been noted that children and elderly individuals should use this botanical product with caution and that pregnant women, infants, and individuals with renal insufficiency are prohibited from using this botanical product. Aristolochiae Herba, which is the aboveground part of Aristolochia and Northern Aristolochia, has beneficial effects on abdominal pain and rheumatism, but the Ch. P 2015 Edition also notes that

[1]Center for Drug Safety Evaluation and Research, Innovation Research Institute of Traditional Chinese Medicine, Shanghai University of Traditional Chinese Medicine, Shanghai 201203, China; [2]Center for Drug Safety Evaluation and Research, State Key Laboratory of Drug Research, Shanghai Institute of Materia Medica, Chinese Academy of Sciences, Shanghai 201203, China and [3]Zhongshan Institute for Drug Discovery, Institutes of Drug Discovery and Development, CAS, Zhongshan 528400, China
Correspondence: Zhong-ping Deng (dzp@shutcm.edu.cn) or Li-kun Gong (lkgong@cdser.simm.ac.cn) or Jin Ren (jren@cdser.simm.ac.cn)
These authors contributed equally: Yong-zhen Liu, Heng-lei Lu

Received: 13 October 2020 Accepted: 6 February 2021
Published online: 8 March 2021

this botanical product has the same contraindications as Aristolochia. Thus, the MRHD of Herba Aristolochiae is limited to 6 g, and the content of AAI should not exceed 0.01%; thus, the MRHD of AAI is limited to 0.6 mg. *Asarum heterotropoides* is a common botanical product used for the treatment of cold, headache, toothache, nasal congestion, rheumatism, and phlegm, but the MRHD is limited to 3 g, and the content of AAI should not exceed 0.001%; thus, the MRHD of AAI is limited to 0.03 mg.

In 2017, AA was first reported to also have an association with hepatocellular carcinoma (HCC), based on the AA exposure-related mutational signature with characteristic A>T transversions at the 5′-CAG-3′ or 5′-CTG-3′ motif widely found in Asian HCC patients, especially those from Taiwan, China [25]. This finding has caused widespread concern worldwide. However, obviously, it cannot be concluded that HCC is directly associated with AA based on the results from this exploratory retrospective survey. First, the tumor tissue was obtained from nonconsecutive patients, and inclusion of HCCs was solely based on the availability of adequate DNA for analysis and was not based on AA exposure history. Moreover, no quantitative data of AA-DNA adducts in these samples from HCC patients were provided. Thus, the characteristic A>T transversion mutation cannot be simply attributed to AA directly, since it is unclear whether these HCC patients had been exposed to AA. On the other hand, the characteristic A>T transversion is not a unique characteristic of AA-induced mutations. Xin et al. investigated the mutational signature of dozens of potential hepatocarcinogens/or their cofactors associated with A>T transversion mutations and found that several environmental or industrial hepatocarcinogens, such as 7,12-dimethylbenz(a)anthracene (DMBA), N-ethyl-N-nitrosourea, and diethylnitrosamine (DEN), induce mutation signatures highly similar to those induced by AA in the liver [26]. Recently, whole-exome sequencing studies revealed that the rates of A>T transversion were more than 60% and ~37.3% for DMBA and DEN exposure, respectively [27–29]. Thus, this survey cannot exclude the possibility that these chemicals might also contribute to the AA-induced mutational signature. Second, this survey did not exclude the potential contributions of other cofactors to the occurrence of HCC. The etiology and pathogenesis of HCC are multifactorial. Genetic disorders, nonalcoholic steatohepatitis, hepatitis B and C virus (HBV/HCV) infection and toxins, including alcohol and aflatoxin B1, are the major risk factors for hepatocarcinogenesis [30, 31]. It has been reported that HBV infection is implicated in the etiology of as many as 80% of HCC cases that occur in Chinese and black African populations [32]. In addition, other environmental hepatocarcinogens (e.g., DMBA) and the disease status of patients needing long-term, concurrent use of other medications may also be confounding factors and contribute to the occurrence of HCC [32–34]. Taken together, these observations indicate that the mutational spectrum of AA exposure is not sufficient to support the above association. In 2018, Chen et al. found that AA may dose-dependently increase the risk for HCC in HBV-infected patients in a retrospective, population-based, cohort study on patients older than 18 years who had a diagnosis of HBV infection [34]. However, the increased risk shown in this analysis could be due to confounding by disease severity, as patients with more severe forms of hepatitis and thus a higher risk of liver cancer would be more likely to receive these herbs. On the other hand, the findings from this study more likely indicated that AA exerts tumor-promoting effects in HCC patients with HBV infection, liver cirrhosis, alcohol-related disease, or nonalcoholic steatohepatitis.

Although the potential association between AAI and HCC has been retrospectively investigated in HCC patients, there is no direct evidence that AA exposure leads to liver cancer in adult animals and humans. Thus, we believe that investigating the association between AA exposure and HCC in sensitive animal models is urgently warranted. Moreover, the potential roles (e.g., promotion or initiation) and genetic events (formation of AA-DNA adducts) underlying AA-induced tumorigenesis should first be further investigated in animals. The purpose of this study was to investigate whether AAI, the major component of AA mixtures, exerts any tumor-initiating or tumor-promoting effect via a sensitive medium-term liver bioassay with several cofactors and to investigate whether AAI can directly induce HCC via a long-term liver bioassay after oral administration in adult rats. Findings from our animal studies will pave the way for further large-scale epidemiological investigations of the associations between AA and HCC.

MATERIALS AND METHODS

Chemicals and materials

8-Methoxy-6-nitrophenanthro-(3,4-d)-1,3-dioxolo-5-carboxylic acid (AAI, purity 98%) was obtained from Nanjing Chunqiu (Nanjing, China). Proteinase K, DNase I, alkaline phosphatase, nuclease P1, RNase A, and RNase T1 were purchased from Sigma-Aldrich (Shanghai, China). Phosphodiesterase I was purchased from Worthington Biochemical Corp. (Shanghai, China). Neutral-buffered formalin (NBF, 10%) was purchased from Sinopharm (Shanghai, China). The DNA adduct 7-(deoxyadenosin-N^6-yl) (dA) aristolactam I (ALI) (dA-ALI) was synthesized as previously described [35, 36]. A ZR FFPE DNA Miniprep Kit (ZM) was purchased from Zymo Research (Beijing, China). A rabbit anti-GST-P pAb was obtained from Medical Biological Laboratories (Tokyo, Japan). An HRP-labeled secondary antibody was purchased from Fujian Maixin (Fuzhou, China). Dimethyl sulfoxide (>99.9%) and ACS reagent-grade formic acid (98%) were purchased from Sinopharm (Shanghai, China). All solvents used for LC-MS/MS were of high purity and were purchased from Merck Chemical.

Synthesis of AAI-derived DNA adducts

DNA adducts, i.e., dA-ALI, were synthesized according to the protocol described by Byeong Hwa Yun with modifications [36]. AAI (20 mg) in dimethylformamide (2 mL) was mixed with 500 mg of Zn powder pretreated with 1% HCl. Then, dA (40 mg) in 50-mM potassium phosphate buffer (20 mL, pH 5.8) was added to the AAI/Zn mixture and incubated at 37 °C for 24 h in the dark, and the reaction was stopped by incubation in an ice bath for 30 min. The nonreacted Zn powder was removed by centrifugation at 15,000 × *g* for 15 min. The supernatant was dried with a nitrogen evaporation system, extracted three times with ethyl acetate, and finally dissolved in 1 mL of methanol.

Detection of AAI-DNA adducts by ultra-performance liquid chromatography–electrospray ionization/multistage mass spectrometry (UPLC–ESI–MS)

Formalin-fixed, paraffin-embedded (FFPE) rat liver, kidney, and stomach samples were sliced from paraffin blocks. The tissues were then processed with a Quick-DNA FFPE Kit (ZM-D3067, Zymo, Beijing, China) following the manufacturer's protocol with minor modifications. The FFPE tissue (one section, 10-μm thick) was pretreated with a deparaffinization solution (400 μL) for 1 min at 55 °C, and tissues were then incubated with 100 μL of digestion buffer containing 10-mM β-ME and proteinase K (200 μg) at 55 °C for 16 h. The lysates were incubated first at 94 °C for 20 min and then with RNase A (5 μL) for 5 min at room temperature. Then, DNA was isolated using a silica spin column following Zymo Research's protocol with minor modifications. The concentration of DNA was determined with a Quant-iT PicoGreen dsDNA Assay Kit (Thermo Fisher, Shanghai, China).

According to the protocol reported by Yun et al. [36], DNA was digested with deoxyribonuclease I (254.2 U/mg DNA) for 1.5 h at room temperature, with nuclease P1 (200 U/mL in 1 mM $ZnCl_2$, 4 U/mg DNA) for an additional 3 h at 37 °C, and with alkaline phosphatase I (24 U/mL in 1 mM $MgCl_2$ buffer, 2 U/mg DNA) and phosphodiesterase I (1.7 U/mL in 110-mM Tris-HCl (pH 8.9), 0.0714

U/mg DNA) for an additional 18 h at 37 °C. After digestion, two volumes of ice-cold ethanol were added to the DNA lysates, and the lysates were incubated on ice for 1 h. The protein pellet and salt were removed by centrifugation at 15,000 × *g* for 5 min. The resulting supernatant solution was dried with a nitrogen evaporation system and redissolved in 100 μL of the mobile phase solution.

AAI-DNA adducts were analyzed in an LC-30A UPLC system (Shimadzu, Japan). Chromatographic separation of the samples was carried out on an Ace Excel C18 column (50 × 2.1, 3 mm; Phenomenex, Torrance, CA, USA). The mobile phase consisted of 0.2% formic acid in water (A) and acetonitrile (B) with a flow rate of 0.4 mL/min at 30 °C. A gradient eluent was delivered to separate the peaks of dA-ALI (the internal control) as follows: 0.01–0.50 min, 90% solvent A and 10% B; 0.51–3.00 min, a linear gradient to 70% B; and 3.00–3.20 min, a linear gradient to 90% B. The mobile phase (10% solvent A and 90% B) was maintained from 3.21 to 4.40 min, and the system was then returned to the initial conditions from 4.41 to 5.00 min. Mass spectrometric detection was performed in an AB SCIEX Triple Quad 6500 system (SCIEX, Shanghai, China) with an electrospray ionization source. The system was operated in positive-ion detection mode with multiple reaction monitoring. Data were acquired and processed using AB SCIEX Analyst 1.61 software (SCIEX, Shanghai, China). The mass spectrometric parameters of each compound are summarized in Supplementary Tables S1 and S2. The source parameters were also optimized as follows: curtain gas and collision gas pressures of 40 and 9 psi, respectively, were used; the ion spray voltage and temperature were maintained at 5000.0 V and 500.0 °C, respectively; and ion source gas 1 and ion source gas 2 were both set to 50 psi.

Animal study design

All animal protocols were reviewed and approved by the Shanghai Institute of Materia Medica Animal Care and Use Committees (IACUC No. 2018-01-RJ-156). Six-week-old male Sprague–Dawley (SD) rats were randomly divided into groups after acclimatization for 5–7 days.

Medium-term study. Ninety-six rats were divided into 14 groups (Figs. 1a, 2a and Table 1) of 6 or 12 animals each. For the initiation assay, a single oral dose of AAI (20, 50, or 100 mg/kg) was administered on Day 1 to evaluate the initiating ability of AAI in the presence and absence of 2-acetylaminofluorene (2-AAF) (AAF^+ and AAF^-, respectively; Fig. 1a). For the promotion assay, doses of 0.1, 1 or 10 mg/kg AAI were administered to the rats (once a day, 5 days a week (Monday to Friday), for a total of 6 weeks) to evaluate its promoting ability in the presence of DEN (DEN^+, Fig. 2a), and doses of 2, 10, or 20 mg/kg AAI were administered to the rats by oral gavage (once a day, 5 days a week (Monday to Friday), for a total of 6 weeks) to test its promoting activity in the absence of DEN (DEN^-, Fig. 2a). A negative control group (1% $NaHCO_3$), DEN control group (DEN^+) and positive control group (DEN^+AAF^+) were also established concurrently. Three weeks after initiation, all rats were subjected to partial hepatectomy (PH), which involved removal of the left and middle lobes of the liver, to stimulate liver proliferation. Eight weeks after initiation, all rats were sacrificed, and the liver and kidney tissues were collected.

Long-term study. A total of 104 rats were randomly divided into four groups (26 rats/group). AAI (0, 0.1, 1, or 10 mg/kg) was administered to SD rats for up to 52 weeks (once a day, 5 days a week (Monday to Friday)). PH was performed 1 week after the first administration of AAI, and the rats were sacrificed at 6, 26, or 52 weeks after the first administration of AAI for the collection of the liver, kidney, stomach, intestine, and any other organs/tissues with gross findings.

Justification for dose level selection. The doses of DEN and 2-AAF used in the medium-term study were selected based on the previous results showing that evident GST-P^+ foci could be induced at the relevant dose levels [37–39]. The dose levels of AAI were selected mainly based on the data provided in the final report on AA (https://ntp.niehs.nih.gov/ntp/roc/twelfth/2010/finalbds/aristolochic_acids_final_508.pdf) by the National Toxicology Program. This report states that 10-mg/kg AA (77.24% AAI and 21.18% aristolochic acid II) was used as the highest dose that could be tolerated for at least 3 months of administration in a 52-week toxicity study in rats and that the half lethal dose (LD_{50}) in male rats after administration by a single oral gavage was 203.4 mg/kg. Therefore, here, the high dose used for repeated administration of AAI was 10 mg/kg for both the medium-term study in the presence of DEN and the long-term study; the high dose in the medium-term study in the absence of DEN was 20 mg/kg, twofold that used in the presence of DEN; and the high dose used for single oral administration was 100 mg/kg, approximately one-half of the LD_{50} value, which was high enough to cause toxic effects but not to induce death in rats. In addition, according to the Ch. P 2015 Edition [23], the MRHD of AAI is limited to 0.6 mg, which is equivalent to 0.06 $mg \cdot kg^{-1} \cdot d^{-1}$ in rats, based on the body surface area. Thus, the high single dose of 100 mg/kg is ~1667-fold the MRHD of AAI, and the doses of 0.1, 1, and 10 mg/kg used in the long-term study are ~1.67-, 16.7-, and 167-fold the MRHD of AAI, respectively. Investigating hepatocarcinogenicity at much wider dose ranges will provide additional information for further large-scale epidemiological investigations of the associations between AA and HCC.

Immunohistochemical staining and analysis of GST-P^+ foci

Rat livers were fixed with NBF and embedded in paraffin. Tissue sections (6 μm) were routinely processed with xylene and a graded alcohol series and stained for GST-P by the ABC method. A rabbit anti-GST-P antibody was obtained from MBL. Affinity-purified, biotin-labeled goat anti-rabbit immunoglobulin G and ABC complex (Vectastain ABC kit) were obtained from Vector Laboratories (Burlingame, CA, USA). Peroxidase binding was visualized by the diaminobenzidine method. The sections were then lightly counterstained with hematoxylin for microscopic examination. Nonimmune γ-globulin was used instead of targeted antibodies as the negative control. The specimens were examined and photographed using a microscope (Leica Aperio, GER). GST-P^+ foci containing more than ten cells per cross section were identified by an image processor and quantified as the numbers per mm^2 of the liver section. The areas of the GST-P^+ foci were measured using HALO image analysis software.

H&E staining and microscopic examination

Tissues from liver, kidney, and gastrointestinal tract were collected at necropsy, fixed with 10% NBF, embedded in paraffin, sectioned (3 μm), and stained with hematoxylin and eosin (H&E) for histological evaluation. Injury and tumor occurrence in the liver, kidney, stomach, and intestine were identified according to previously reported criteria [40–42]. The slides were analyzed by a second experienced pathologist with FRCPath and FIATP certification.

Statistical analysis

The data are presented as the mean ± SEM values. Statistical analysis was performed by unpaired, two-tailed *t* test or one-way ANOVA followed by the Tukey's or Dunnett's multiple comparison test. $P < 0.05$ was considered statistically significant. GraphPad Prism 8.1.1 (GraphPad Prism Software Inc., San Diego, CA, USA) was used for data calculation, statistical analysis, and graph generation.

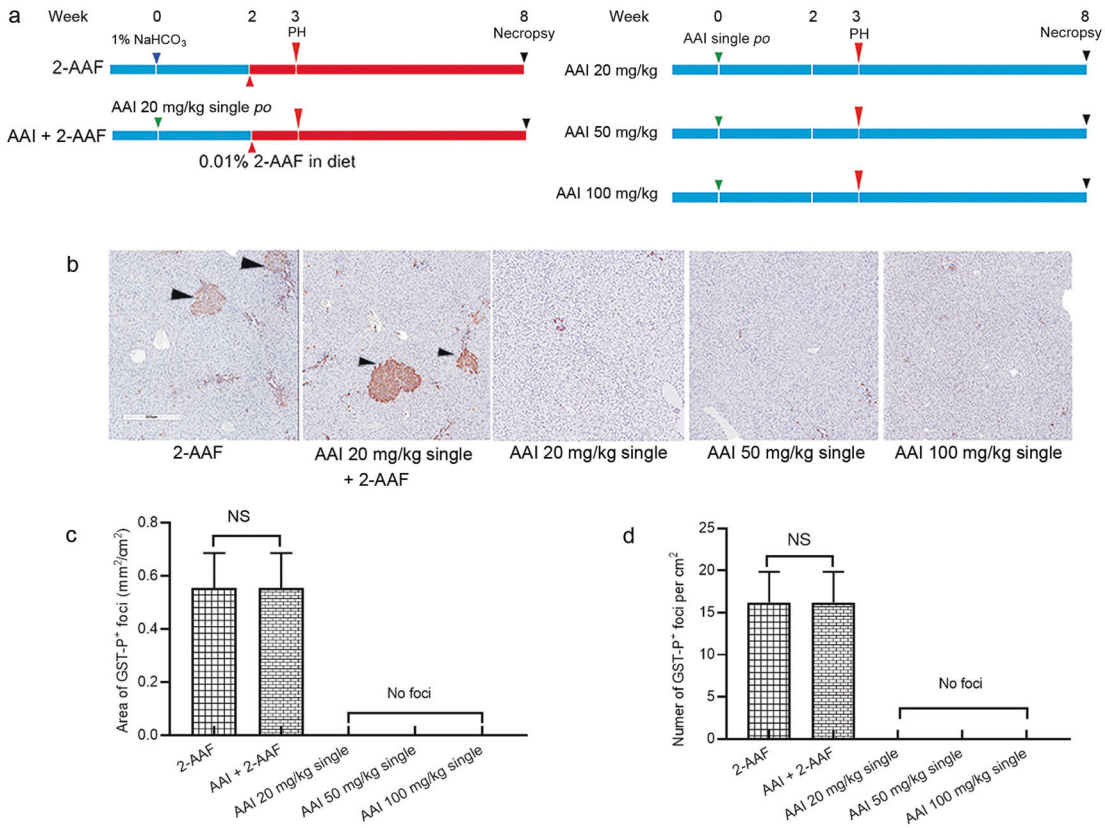

Fig. 1 A single dose of AAI did not initiate clonal expansion in the liver or enhance those induced by 2-AAF. A single dose of AAI was administered to SD rats by oral gavage. **a** Schematic diagram of the study design. PH: partial hepatectomy. **b** Representative images of GST-P$^+$ foci in each group. Scale bar: 500 μm. Arrowheads indicating the GST-P positive foci. **c, d** The number and area of GST-P$^+$ foci analyzed by HALO software. Foci containing ten or more cells were measured and included in the statistical analysis. No foci: no typical GST-P$^+$ foci in the liver section. The number and area of GST-P foci are presented as the mean ± SEM and statistically analyzed by unpaired, two-tailed *t* test. NS: no statistically significant difference. The number of animals in each group is listed in Table 1.

RESULTS

Single oral administration of AAI did not induce clonal expansions or enhance those elicited by 2-AAF

2-AAF is a potent genotoxic liver carcinogen in rats, and the genotoxic reactivity of its metabolites results in the formation of 2-AAF-DNA adducts. In addition to having genotoxic effects, 2-AAF causes a variety of nongenotoxic tumor-promoting alterations that lead to uncontrolled and unrestricted proliferation of initiated cells. Placental form GST (GST-P) is mainly found in the placenta and tumor tissues. It has been used as a sensitive marker for visualizing and quantitatively analyzing preneoplastic lesions in the liver, kidney, colon, and other organs [37, 38, 43]. To evaluate the potential initiating activity of AAI, a single dose of AAI (20, 50, or 100 mg/kg) was administered to SD rats with or without subsequent administration of the known promotor 2-AAF (Fig. 1a). Analysis of GST-P$^+$ foci indicated that 2-AAF alone promoted the development of GST-P$^+$ foci (Fig. 1b–d), as expected. There was no statistically significant difference in the number or area of GST-P$^+$ foci between the 2-AAF alone and AAF$^+$AAI (20 mg/kg) groups. No typical GST-P$^+$ foci were noted after a single oral administration of AAI at a dose of 20, 50, or 100 mg/kg in the absence of 2-AAF (Fig. 1b–d).

Repeated oral administration of high-dose AAI promoted clonal expansion in the liver

In the medium-term study, AAI was administered to SD rats for 6 weeks to assess its promoting effects; DEN was used as an initiator, and 2-AAF was used as a positive control promoter (Fig. 2a). Typical and large GST-P$^+$ foci were noted in the positive control (DEN$^+$AAF$^+$) group, with a mean number of 76.4 ± 6.31 foci/cm^2 and a mean area of 4.88 ± 1.42 mm^2/cm^2 (Fig. 2b–d). When 2-AAF was replaced with AAI as a promotor in this protocol, the number and area of GST-P$^+$ foci in the DEN$^+$AAI (10 mg/kg) group increased ($P < 0.01$ and $P < 0.05$, respectively) compared to those in the DEN$^+$ group but decreased markedly ($P < 0.0001$, Fig. 2b–d) compared to those in the DEN$^+$AAF$^+$ group. There was no statistically significant increase in the number or area of GST-P$^+$ foci in the DEN$^+$AAI (0.1 and 1 mg/kg) groups compared to the DEN$^+$ group. No typical GST-P$^+$ foci were observed in the negative control group or in the DEN$^-$AAI (2, 10, and 20 mg/kg) groups (Fig. 2b–d).

In the long-term study, AAI (0.1, 1, and 10 mg/kg) was orally administered to SD rats subjected to PH for up to 52 weeks. Animals were necropsied at the end of Weeks 6, 26, and 52 (Fig. 3a), and preneoplastic lesions/clonal expansion in the liver were assessed. GST-P$^+$ foci analysis indicated that 10-mg/kg AAI increased the number and area of GST-P$^+$ foci in a time-dependent manner and had a significant effect from Weeks 16–26 ($P < 0.05$ and $P < 0.01$, respectively) onwards; there was no significant increase in the number or area of GST-P$^+$ foci in the other AAI (0.1 or 1 mg/kg)-treated groups compared to the concurrent control group at Weeks 6, 26, or 52 (Fig. 3b–d).

AAI caused rat death and induced carcinogenesis in the forestomach, intestine, and kidney but not in the liver

Chronic activation of the wound healing response is a driving force for the development of HCC. Therefore, in this study, AAI (0.1, 1, or 10 mg/kg) was administered to SD rats by oral gavage

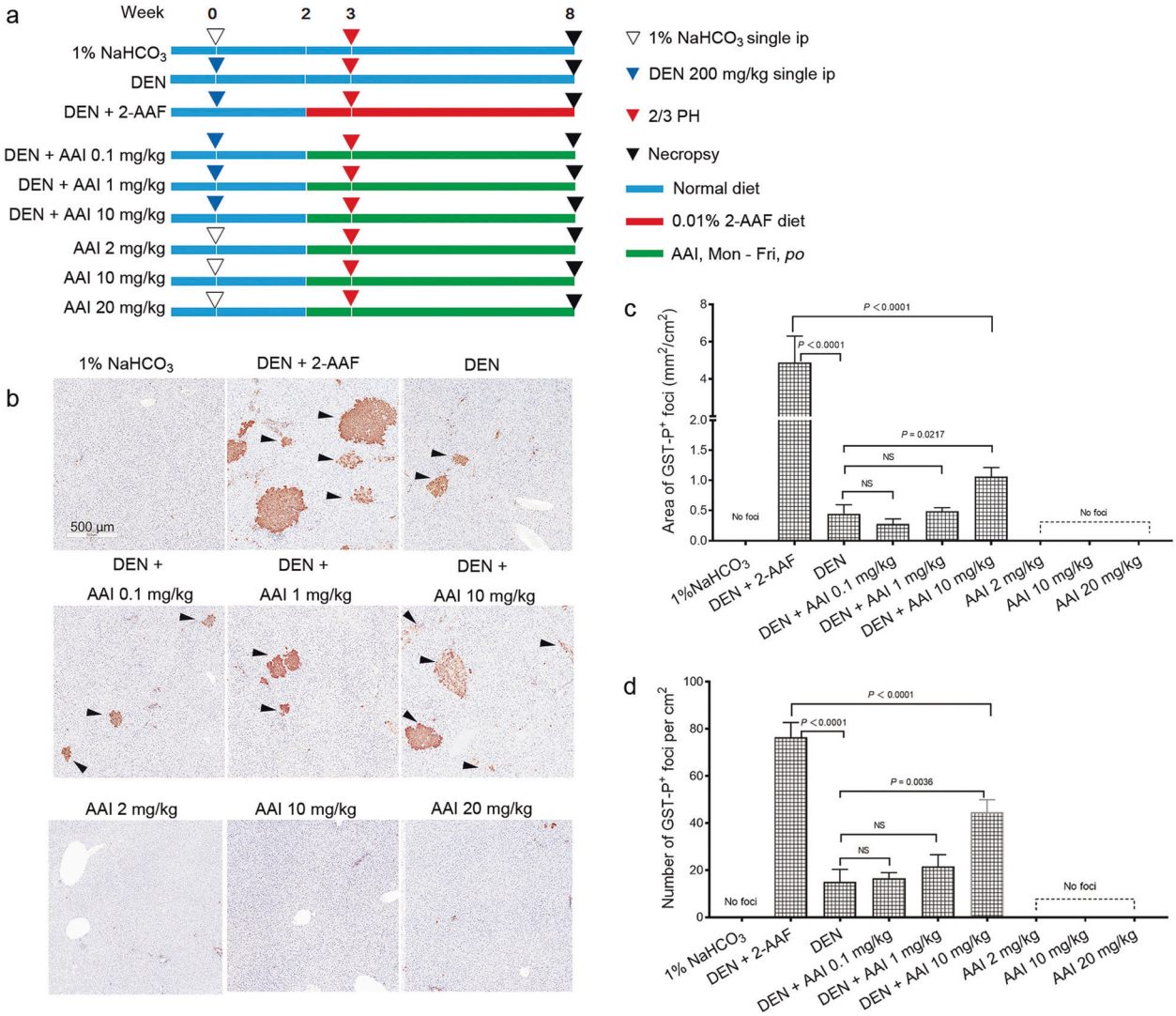

Fig. 2 Repeated administration of AAI promoted clonal expansion initiated by DEN in the liver. a Schematic diagram of the study design. AAI was administered by oral gavage (once a day from Monday to Friday for a total of 6 weeks) 2 weeks after DEN initiation. 2/3PH: two-thirds partial hepatectomy. **b** Representative images of GST-P$^+$ foci in each group. Scale bar: 500 μm. Arrowheads indicating the GSP-P positive foci. **c, d** The number and area of GST-P$^+$ foci analyzed by HALO software. Foci containing more than ten cells were measured and included in the statistical analysis. No foci: no typical GST-P$^+$ foci were noted in the liver section. The number and area of GST-P foci are presented as the mean ± SEM and statistically analyzed by unpaired, two-tailed *t* test or one-way ANOVA followed by the Tukey multiple comparison test. NS: no statistically significant difference. The number of animals in each group is listed in Table 1.

for up to 52 weeks, and PH was performed one week after the first administration of AAI to activate the wound healing response/cell proliferation response and investigate the potential carcinogenicity of AAI in this liver microenvironment (Fig. 4a).

AAI caused death in a time- and dose-dependent manner in the 52-week study (Fig. 4b). No animal had died by the end of Week 6. By the end of Week 26, the mortality rates in the 0, 0.1, 1.0, and 10-mg/kg AAI-treated groups were 0%, 0%, 0%, and 50% (from Week 16 onwards), respectively. By the end of Week 52, the mortality rates were 0%, 20% (Week 38), 100% (Weeks 29–44), and 100% (Weeks 16–30) in the 0, 0.1, 1, and 10-mg/kg AAI-treated groups, respectively.

In the liver, hepatocyte necrosis, including single cell necrosis, focal necrosis, and/or bridging necrosis, was observed at Weeks 16–52 in the 10-mg/kg group and at Weeks 26–52 with 1-mg/kg AAI (Fig. 4c, d and Supplementary Fig. S1) but was not observed in the 0.1-mg/kg group throughout the study. However, no nodules or HCC were observed in any AAI-treated group upon macroscopic or microscopic examination throughout the 52-week period of the study (Fig. 4c, d and Supplementary Fig. S1).

AAI caused carcinogenesis in the forestomach, intestine, and kidney (Fig. 5 and Supplementary Fig. S2). Severe squamous carcinoma of all pathological stages (from hyperplasia to carcinoma) in the forestomach was observed in all AAI-treated groups (0.1, 1, and 10 mg/kg) in a time- and dose-dependent manner. These squamous cell carcinomas were characterized by an endophytic growth pattern with penetration of the muscularis mucosae and a disorganized squamous epithelium with inconsistent keratinization. Intestinal sarcoma was induced by the medium and high doses of AAI (1 and 10 mg/kg). These intestinal sarcomas were characterized by pleomorphism, spindle-shaped and/or blunt-ended hyperchromatic nuclei, fibrillary cytoplasm, indistinct cell borders, and a high mitotic index. Kidney tubular adenomas were elicited by the high dose of AAI. These kidney tubular adenomas were clearly circumscribed, with compression of the surrounding parenchyma and further characterized by irregular

Table 1. DNA adduct levels in liver and kidney after single or 6-week repeated dosing of AAI.

Treatment	AAI dose (mg/kg)	Number of animals	dA-ALI in liver (/10^6 nucleotides)	dA-ALI in kidney (/10^6 nucleotides)	dA-ALI in liver relative to that in kidney (%)
1% $NaHCO_3$	0	8	BLQ	BLQ	NA
DEN + 2-AAF	0	10	BLQ	BLQ	NA
DEN	0	5	BLQ	BLQ	NA
DEN + AAI (repeated)	0.1	6	BLQ	BLQ	NA
	1	6	3.9 ± 0.6	6.3 ± 0.3	62%
	10	11	19.5 ± 1.6	50.2 ± 6.8	39%
AAI (repeated)	2	5	8.3 ± 1.0	7.0 ± 1.4	119%
	10	6	21.6 ± 5.2	43.5 ± 8.6	50%
	20	3	62.6 ± 4.9**	99.3 ± 10.2##	63%
2-AAF	0	6	BLQ	BLQ	NA
2-AAF + AAI (single)	20	6	BLQ	1.7 ± 0.5	NA
AAI (single)	20	6	BLQ	1.5 ± 0.4	NA
	50	6	0.6 ± 0.1	5.5 ± 0.9	11%
	100	5	1.5 ± 0.3	13.4 ± 2.0	11%

DEN: 200 mg/kg, single ip injection on Day 1; 2-AAF: 0.01% fed with diet from Day 15 to Day 56; AAI (repeated): AAI with the indicative doses was orally administered for 6 weeks (once a day from Monday to Friday); AAI (single): AAI with the indicative doses was orally administered on Day 1; all rats were sacrificed on Day 56.
BLQ: below the limit of quantification, *NA:* not applicable.
$^{**}P < 0.01$vs. dA-ALI in liver at AAI 100 mg/kg (single dose) by unpaired, two-tailed *t* test.
$^{\#\#}P < 0.01$ vs. dA-ALI in kidney at AAI 100 mg/kg (single dose). % = 100 × (dA-ALI in liver/dA-ALI in kidney).

to nodular growth patterns and well-differentiated tubules. The development of tumors in the forestomach, intestine, and kidney was considered to be the primary cause of death in the rats.

AAI promoted the accumulation of DNA adducts in the kidney, liver, and stomach in a dose- and time-dependent manner

Cellular nitroreductases activate AAI, producing reactive intermediates, and binding covalently to dA and 7-(deoxyguanosin-N^2-yl) (dG) residues in DNA to form the aristolactam DNA adducts dA-ALI and dG-ALI [36]. These mutagenic lesions can generate a unique Tp53 mutation spectrum dominated by A:T>T:A transversions with mutations at dA residues located almost exclusively on the nontranscribed strand [44, 45]. A validated UPLC–ESI–MS method was used to determine the levels of dA-ALI in the liver, kidney, and stomach and to assess the relationship between dA-ALI accumulation and toxicity/carcinogenesis in the liver, stomach, and kidney.

In the medium-term study, single and repeated oral administration of AAI resulted in accumulation of dA-ALI both in the liver and in the kidney in a dose-dependent manner (Fig. 6a, b and Table 1). A much greater quantity of DNA adducts accumulated in the liver and kidney in the repeated administration groups than in the single administration groups. However, generally, there was less DNA adduct accumulation in the liver than that in the kidney at the same AAI dose level.

Similarly, treatment with AAI for up to 52 weeks resulted in DNA adduct accumulation in the liver, kidney, and stomach in a time- and dose-dependent manner (Fig. 6c–e and Table 2). DNA adduct accumulation was highest in the kidney, second-highest in the liver, and lowest in the stomach. The mean levels of dA-ALI in the liver and stomach were 21%–48% and 0.5%–5% of those in the kidney, respectively, after 27–52 weeks of AAI treatment (Fig. 6c–e and Table 2). The dA-ALI levels in the 10-mg/kg AAI-treated group were lower during Weeks 27–52 than during Weeks 16–26; this decrease might be related to the cessation of AAI administration at Week 16 due to the poor health status of the animals in this group.

DISCUSSION

Since the first demonstration that chemicals in coal tar cause cancer in animals, rodent models of chemical carcinogenesis have led to the research concept of multistage tumor development involving initiation, promotion, and progression stages [46]. A medium-term rat liver bioassay system based on this concept of chemical carcinogenesis was established by Nobuyuki Ito and is used as an alternative approach to the conventional 2-year bioassay system described by ICH guideline S1B [37–39]. This system involves the treatment of rats with genotoxic DEN to initiate hepatocarcinogenesis and subsequent dietary exposure to a test substance. DEN causes mutations at specific locations in the genome. Then, a variety of selective processes, including microenvironment-related events at the levels of metabolism and DNA repair, lead to eventual survival and clonal expansion of initiated cells with a specific set of mutations [46–48]. On the other hand, tumor promoters can also function by nonmutational mechanisms to stimulate mitotic signaling pathways, depending on the exposure concentration and duration. This initiation–promotion process is particularly typical in skin with phorbol esters and in the liver with phenobarbital as the promoter [46, 49]. Even though carcinogenesis has been characterized by ten essential hallmarks of cell physiology [50], the initiation–promotion model still has important explanatory and predictive power for the carcinogenicity of test chemicals [46, 48] and is recommended by the ICH as a component of safety evaluations of pharmaceuticals [51]. In the present medium-term study, we found for the first time that AAI exerted weak promoting effects on preneoplastic hepatic lesions initiated by DEN. Several lines of evidence support this finding. First, repeated administration of AAI increased the number and area of GST-P^+ foci initiated by DEN but did not induce any typical foci in the absence of DEN. However, the promoting effect of AAI was markedly weaker than that of 2-AAF. Second, a single dose of AAI did not change the foci formation pattern of 2-AAF, which can induce preneoplastic lesions without an initiating stimulus, and a single high dose of AAI (100 mg/kg) alone did not induce any typical GST-P^+ foci

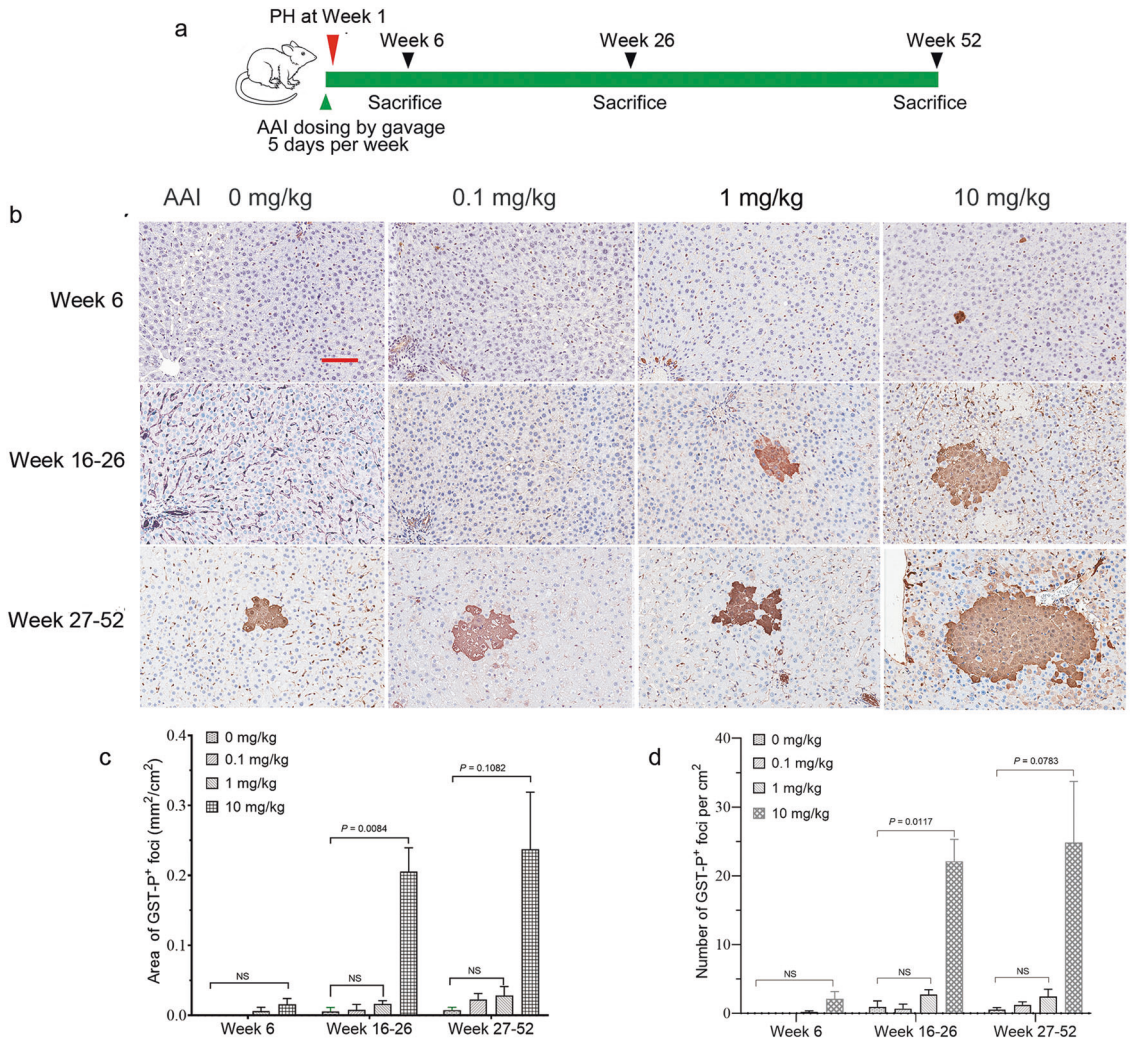

Fig. 3 AAI promoted the development of clonal expansion in the liver. a Schematic diagram of the study design. **b** Representative images of GST-P$^+$ foci in each group. Scale bar: 100 μm. **c, d** The number and area of GST-P$^+$ foci are presented as the mean ± SEM and statistically analyzed by one-way ANOVA followed by the Dunnett's multiple comparison test. NS: no statistically significant difference.

similar to those elicited by DEN or 2-AAF. Third, accompanied by the accumulation of AAI-DNA adducts, the mutational hotspot Tp53 did not show an increase in A:T>T:A transversions, a mutational signature of AA exposure, strongly indicating the role of nonmutational action mechanisms in the promotion effect of AAI in the liver (Supplementary file, Supplementary Tables S3 and S4).

It has been confirmed that AA can induce renal toxicity and is the etiological agent of aristolochic acid nephropathy (AAN) and Balkan endemic nephropathy (BEN) [12–17, 19–22, 52, 53]. Epithelial carcinoma of the urethra is the major cancer induced by AA and occurs with a high prevalence in patients with AAN or BEN [53]. However, no data have shown that HCC occurs in patients with AAN or BEN. In 2017, AA was first reported to also have an association with HCC in Chinese and Southeast Asian populations based on the characteristic AA mutation—A:T>T:A transversion—found in some HCC patients [25]. However, it cannot be concluded that AA is the etiological agent of HCC due to a lack of evidence regarding AA exposure or interference of other cofactors (e.g., HBV infection). In a recent 52-week animal study, Lu et al. reported that in juvenile mice, intraperitoneal injection of AAI (2.5 and 5 mg/kg, equivalent to 1.25 and 2.5 mg/kg, respectively, in rats, based on body surface area) induced visible HCC and combined hepatocellular and intrahepatic cholangiocarcinoma but did not induce tumors in any other organ [44]. This study was a rapid experimental approach to identify hepatic carcinogens. AA is a known carcinogen that can theoretically induce cancers or solid tumors in organs or tissues after metabolic activation. AAI is primarily metabolically detoxified by CYP1As (especially CYP1A2) in humans and rodents [8, 54, 55]. CYP1As have been found to play a critical role in suppressing the carcinogenic and nephrotoxic effects of AAI [19, 56–61]. It has been reported that the activity and mRNA expression levels of CYP1A2 in the livers of juvenile mice are much lower than those in the livers of adult mice [61]. Hence, the results obtained from intraperitoneal injection in juvenile mice might not be appropriate for direct translation to adults.

Mengs reported that oral administration of AA (0.1, 1.0, and 10 mg/kg AA; 77.24% AAI, 21.18% aristolochic acid II) induced tumors in the forestomach, kidney, and bladder but not the liver in a traditional long-term carcinogenicity study in adult Wistar rats [62]. Several other studies have also demonstrated that repeated exposure or acute high-dose exposure induced other tumors but not HCC in adult rodents [63, 64]. In our study, we used a sensitive liver bioassay to further determine whether AAI can directly induce HCC in adult rats after long-term exposure. In this long-

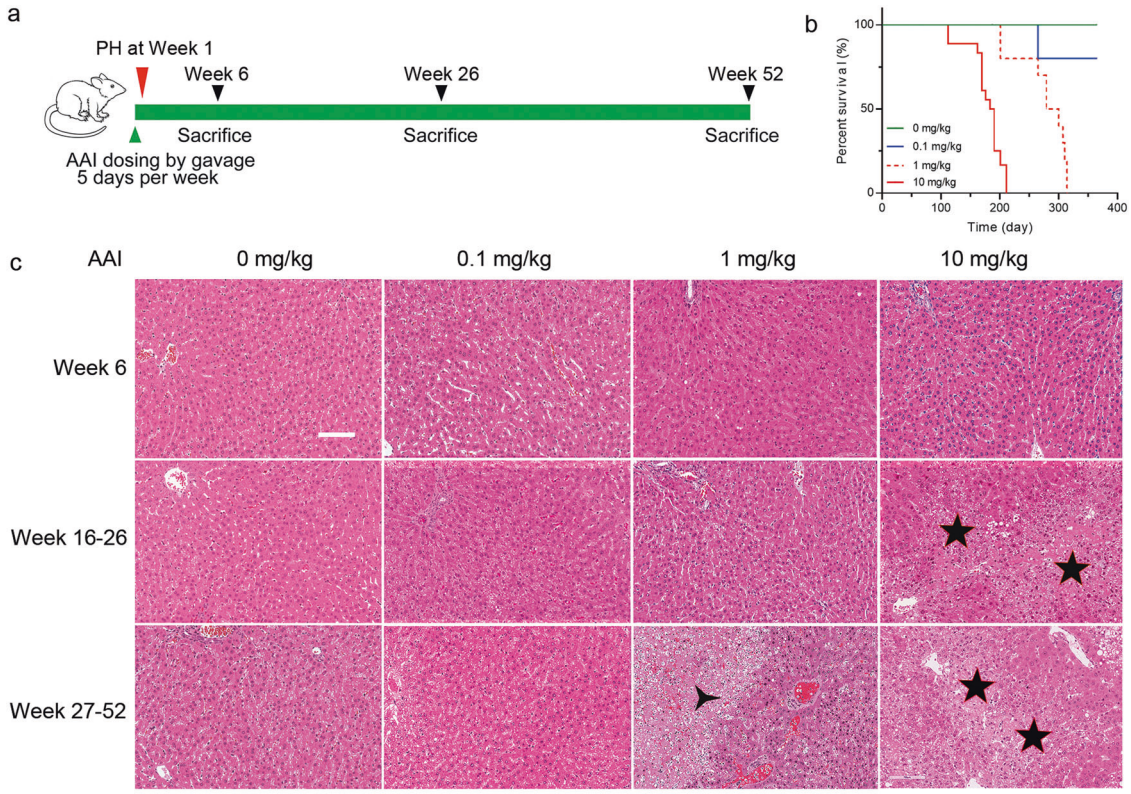

d

Time points	Week 6				Week 16-26				Week 27-52			
Dose (mg/kg)	0	0.1	1	10	0	0.1	1	10	0	0.1	1	10
Single cell necrosis	0/6	0/6	0/6	0/6	0/10	0/9	0/10	2/9	0/9	0/8	1/8	2/6
Focal necrosis	0/6	0/6	0/6	0/6	0/10	0/9	0/10	3/9	0/9	0/8	2/8	1/6
Bridge necrosis	0/6	0/6	0/6	0/6	0/10	0/9	0/10	3/9	0/9	0/8	2/8	1/6

Fig. 4 AAI induced liver injury in the 52-week. a Schematic diagram of the study design. **b** Survival curve of the animals subjected to partial hepatectomy. **c** Representative microscopy images of H&E-stained livers. **d** Summary of necrotic injury in the liver. Stars indicating the bridge necrosis characterized by necrosis confluent involving more than one zone within the lobule and extend zonally from one lobule to another adjacent lobule. Arrowhead indicating the focal necrosis characterized by necrotic hepatocyte with hypereosinophilic cytoplasm, which involving larger groups of hepatocytes within a lobule. Other images show the normal structure of liver. Scale bar: 100 μm.

term study, PH was performed 1 week after the first administration of AAI to activate the wound healing response/cell proliferation response and investigate the potential carcinogenicity of AAI in this microenvironment. Hepatocyte necrosis in the 1 and 10-mg/kg groups and marked increases in the number and area of hepatic GST-P$^+$ foci in the 10-mg/kg group were observed. Similarly, no nodules or HCC tumors in the liver were observed in any AAI-treated group, even in the presence of dA-ALI adducts. On the other hand, squamous carcinoma of the forestomach in all AAI-treated groups (0.1, 1, or 10 mg/kg), intestinal sarcoma in the 1 and 10-mg/kg groups, and kidney tubular adenomas in the 10-mg/kg group were observed. Using this sensitive liver assay, we demonstrated for the first time that AAI promoted clonal expansion (as indicated by GST-P$^+$ foci) in the liver in adult rats. However, the clonal expansion in this long-term study did not progress to nodules or HCC before the rats died from tumors that developed in the forestomach, intestine, and/or kidney. Higashi and his colleagues reported that the clonal expansion of GST-P$^+$ foci is closely related to tumor susceptibility but not directly associated with final malignant transformation, as evidenced by extensive genetic linkage analyses of the carcinogen-resistant rat strain DRH [29, 65–67]. Recently, Li et al. reported that AA exposure considerably accelerated somatic mutation accumulation and enhanced clonal expansion in morphologically normal human urothelium (MNU) in patients with UCC [68]. Chromatin remodeling-related genes, such as KMT2D and KDM6A, were frequently mutated in MNU, whereas canonical driver genes of UCC, such as PIK3CA and FGFR3, were rarely mutated. Their finding implies that acquisition of copy-number alterations occurs late in clonal expansion in the urothelium and that genomic stability is a choke point for final malignant transformation. Our findings that tumors developed in organs other than the liver in adult rats after long-term oral administration (the most common route of human exposure) of AAI were highly consistent with those reported by Mengs et al. [62–64] but completely different from those reported by Lu [44]. The different study designs (juvenile animals vs. adult animals, intraperitoneal injection vs. oral gavage) and the metabolic differences subsequently induced may have contributed to the different hepatic effects observed by Lu et al. (including our team, as reported in this study).

As expected, AA-induced carcinogenesis occurred only in the kidney although the AAI-DNA adduct dA-ALI was detected in both the kidney and liver in the long-term study. It has been reported that hepatic microsomal cytochrome P450 enzymes (e.g., CYP1A2 and CYP1A1) and NQO1 are the major enzymes involved in AAI metabolism and that CYP1A2 is mainly expressed in the liver, while NQO1 is expressed at high levels in urothelial tissue and the kidney [8, 20, 57]. CYP1As (especially CYP1A2) are

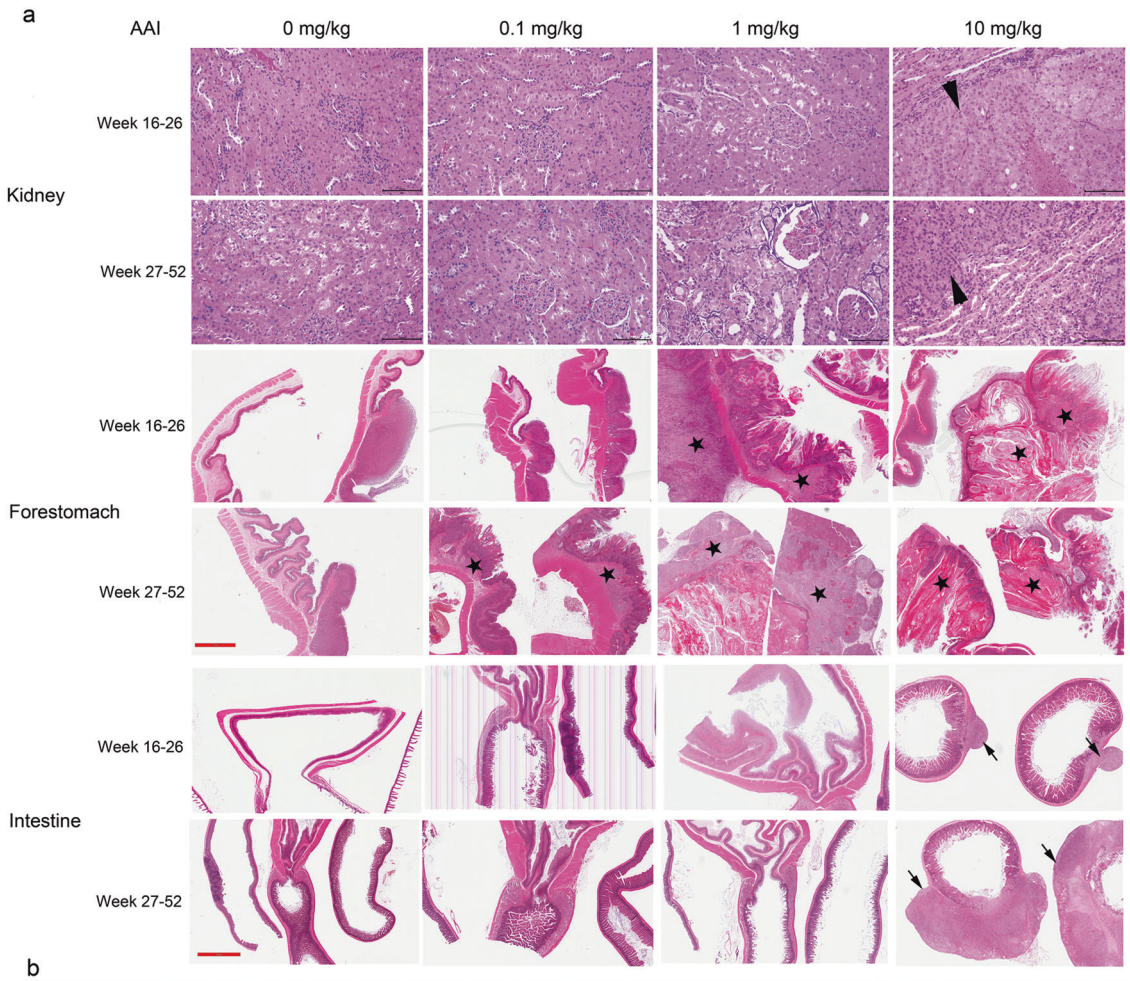

b

Weeks	6				16-26				27-52				16-52			
Dose (mg/kg)	0	0.1	1	10	0	0.1	1	10	0	0.1	1	10	0	0.1	1	10
Forestomach-squamous cell hyperplasia	0/6	0/6	0/6	0/6	0/10	0/9	0/10	1/9	0/9	2/8	0/8	5/6	0/19	2/17	0/18	6/15
Forestomach-squamous cell papilloma	0/6	0/6	0/6	0/6	0/10	0/9	4/10	2/9	0/9	3/8	0/8	0/6	0/19	3/17	4/18	2/15
Forestomach-squamous cell carcinoma	0/6	0/6	0/6	0/6	0/10	0/9	6/10	6/9	0/9	1/8	8/8	1/6	0/19	1/17	14/18	7/15
Intestine-sarcoma	0/6	0/6	0/6	0/6	0/10	0/9	0/10	7/9	0/9	0/8	2/8	3/6	0/19	0/17	2/18	10/15
Kidney-adenoma	0/6	0/6	0/6	0/6	0/10	0/9	0/10	1/9	0/9	0/8	0/8	1/6	0/19	0/17	0/18	2/15

Fig. 5 AAI caused carcinogenesis in the forestomach, intestine, and kidney in the 52-week study. AAI was administered to SD rats by oral gavage (once a day from Monday to Friday for up to 52 weeks). **a** Representative H&E-stained microscopic images of the kidney (scale bar: 100 μm, arrowheads indicating the adenoma), forestomach (scale bar: 2 mm, stars indicating the squamous cell carcinoma), and intestine (scale bar: 4 mm, arrows indicating the sarcoma). **b** Summary of the tumor incidences in the forestomach, intestine, and kidney.

involved in the detoxification of AAI by demethylation to 8-hydroxyaristolochic acid I (AAIa) under aerobic conditions in humans and rodents [8, 19, 57, 69]. CYP1As have been found to play a critical role in suppressing the carcinogenic and nephrotoxic effects of AAI [8, 19, 57–60]. Alternatively, in the cytosol of liver and kidney cells, the nitro group of AAI can be enzymatically reduced by NQO1 to generate ALI [70, 71]. The cyclic nitrenium ion of the nitroreduction intermediate interacts with the exocyclic amino groups of deoxyadenosine and deoxyguanosine residues in DNA to form DNA adducts [72–74]. Furthermore, AAI possesses the chemical characteristics of a substrate for organic anionic transporters (OATs) [70]. Therefore, the OAT family is considered to be one of the pivotal determinants mediating the accumulation of AAI in renal proximal tubules [54]. OATs, especially OAT1 and OAT3, in the basolateral membrane of proximal tubules facilitate the uptake of AAI by renal cells, which at least partially leads to site-selective AAI-induced nephrotoxicity [21, 54, 75–77]. In addition, the phase II metabolite of AAI, sulfate-conjugated ALI, is reported to be transported into the kidney via OAT1, OAT3, and OAT4 [77]. Collectively, these factors might have contributed to the higher AAI-DNA adduct accumulation in the kidney than in the liver and may also be factors affecting the differential susceptibility of the kidney and liver to AAI [78]. Surprisingly, the lowest accumulation of dA-ALI was observed in the forestomach relative to the kidney and liver. However, squamous carcinoma of the forestomach exhibited the earliest occurrence and most rapid progression of all malignancies in all AAI-treated groups (0.1, 1.0, and 10 mg/kg). This pattern might be related to the following aspects: first, the adducts in the forestomach were markedly diluted due to the

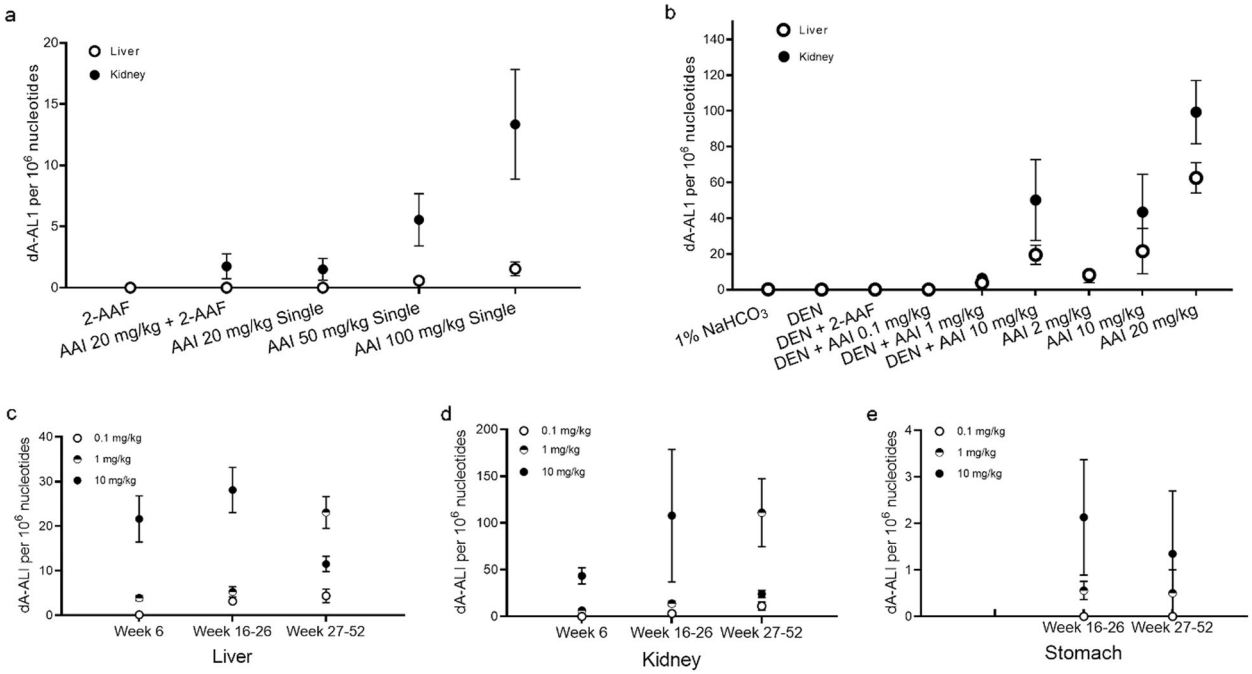

Fig. 6 DNA adduct levels in the liver, kidney, and stomach after AAI treatment. a dA-ALI levels in the liver and kidney in the presence or absence of 2-AAF after a single administration of AAI. **b** dA-ALI levels in the liver and kidney in the presence or absence of DEN after repeated administration of AAI for 6 weeks. The number of animals in each group is listed in Table 1. **c–e** dA-ALI levels in the liver, kidney, and stomach after repeated administration for 52 weeks. The number of animals per group is listed in Table 2.

Table 2. DNA adduct levels in liver, kidney, and stomach in the 52-week repeated-dose study.

Organs	Time	dA-ALI/10^6 nucleotides (mean ± SEM (*n*))			dA-ALI in liver or stomach relative to that in kidney (%)		
		0.1 mg/kg	1 mg/kg	10 mg/kg	0.1 mg/kg	1 mg/kg	10 mg/kg
Liver	Week 6	0.1 ± 0.0 (6)	3.9 ± 0.6 (6)	21.6 ± 5.2 (6)	100%	62%	50%
	Weeks 16–26	3.1 ± 0.4 (9)	5.3 ± 1.2 (8)	28.1 ± 5.1 (6)	100%	38%	26%
	Weeks 27–52	4.4 ± 1.5 (5)	23.1 ± 3.5 (8)	11.5 ± 1.7 (5)	40%	21%	48%
Stomach	Weeks 16–26	BLQ (10)	0.6 ± 0.2 (10)	2.1 ± 1.2 (5)	NA	4%	2%
	Weeks 27–52	BLQ (7)	0.5 ± 0.5 (8)	1.3 ± 1.3 (4)	NA	0.5%	5%
Kidney	Week 6	0.1 ± 0.0 (6)	6.3 ± 0.3 (6)	43.5 ± 8.6 (6)	NA	NA	NA
	Weeks 16–26	3.1 ± 0.5 (9)	13.8 ± 2.5 (10)	107.9 ± 70.7 (6)	NA	NA	NA
	Weeks 27–52	11.1 ± 4.4 (5)	111 ± 36.4 (8)	24.1 ± 3.7 (6)	NA	NA	NA

% = 100 × (dA-ALI in liver/dA-ALI in kidney) or 100 × (dA-ALI in stomach/dA-ALI in kidney).
NA: not applicable, *BLQ:* below the limit of quantification.

unrestricted cell proliferation in the growing tumors [79]; second, long-term local irritation by oral gavage resulted in inflammation and injury, which led to increased sensitivity to AAI; third, AAI might be a genotoxic carcinogen in the forestomach and can cause forestomach cancers even with only a small amount of dA-ALI [80, 81]; fourth, other mechanisms (e.g., epigenetic mechanisms) might be involved in the occurrence of forestomach cancers.

Until the 2020 edition of the Ch. P, only one botanical product containing trace amounts of AA, namely, *Asarum heterotropoides*/Xixin, was included in the Ch. P, and an MRHD of 3 g with a maximal content of AAI not exceeding 0.001% is recommended [82]. Accordingly, the MRHD of AAI in humans is 0.03 mg, which is equivalent to 0.003 $mg \cdot kg^{-1} \cdot d^{-1}$ in rats, based on body surface area. The highest doses used in the medium-term and long-term studies were 100 mg/kg (single dose) and 10 mg/kg (repeated dose), respectively, which are ~33333-fold and 3333-fold the MRHD of AAI in the Ch. P 2020 Edition, respectively. Under the current experimental conditions, no HCC was observed after single-dose administration of AAI at doses of up to 100 mg/kg or after repeated-dose administration of AAI at doses of up to 10 mg/kg for up to 52 weeks. However, AAI promoted the development of clonal expansion initiated by DEN. The etiology and pathogenesis of HCC are multifactorial. Aspects of disease status, such as genetic disorders, nonalcoholic steatohepatitis, HBV/HCV infection, and exposure to other environmental toxins, including alcohol, aflatoxin B1, DEN, etc., are major risk factors for hepatocarcinogenesis. Thus, more attention should be devoted to the interactions between AAI and these cofactors when AAI is used for disease treatment.

In conclusion, AAI promoted clonal expansion in the liver only at a high dose of 10 mg/kg in adult rats, but these lesions had

not progressed to HCC even in the presence of AAI-DNA adducts at the end of the study or until death caused by cancers that developed in the forestomach, intestine, and/or kidney. Findings from our animal studies will pave the way for further large-scale epidemiological investigation of the associations between AA and HCC.

ACKNOWLEDGEMENTS

This work was supported by the National Science and Technology Major Project (2018ZX09101002-002, 2018ZX09201017-004, 2012ZX09301).

AUTHOR CONTRIBUTIONS

LKG, JR, and XMQ were responsible for the study conception and design; XMQ and GZX were responsible for the method validation and sample analysis of AAI-DNA adducts; YZL and XMQ established the in vivo liver PH model; PY, XW, LL, FFY, and XLD performed the ex vivo and in vivo experiments; HLL performed the pathological analysis and data accuracy and integrity check; YZL performed the statistical analysis, drafted and finalized the manuscript with input from all other authors; and ZPD and ZAZ critically reviewed and revised the manuscript.

ADDITIONAL INFORMATION

Supplementary information The online version contains supplementary material available at https://doi.org/10.1038/s41401-021-00622-7.

Competing interests: The authors declare no competing interests.

REFERENCES

1. Anandagoda N, Lord GM. Preventing aristolochic acid nephropathy. Clin J Am Soc Nephrol. 2015;10:167–8.
2. Hsin YH, Cheng CH, Tzen JT, Wu MJ, Shu KH, Chen HC. Effect of aristolochic acid on intracellular calcium concentration and its links with apoptosis in renal tubular cells. Apoptosis. 2006;11:2167–77.
3. Wu TK, Wei CW, Pan YR, Cherng SH, Chang WJ, Wang HF, et al. Vitamin C attenuates the toxic effect of aristolochic acid on renal tubular cells via decreasing oxidative stress mediated cell death pathways. Mol Med Rep. 2015;12:6086–92.
4. Yang L, Li XM, Wang HY. Possible mechanisms explaining the tendency towards interstitial fibrosis in aristolochic acid-induced acute tubular necrosis. Nephrol Dial Transpl. 2007;22:445–56.
5. Zeniya M, Mori T, Yui N, Nomura N, Mandai S, Isobe K, et al. The proteasome inhibitor bortezomib attenuates renal fibrosis in mice via the suppression of TGF-beta1. Sci Rep. 2017;7:13086.
6. Lu H, Bai Y, Wu L, Hong W, Liang Y, Chen BC, et al. Inhibition of macrophage migration inhibitory factor protects against inflammation and matrix deposition in kidney tissues after injury. Mediat Inflamm. 2016;2016:2174682.
7. Nedelko T, Arlt VM, Phillips DH, Hollstein M. TP53 mutation signature supports involvement of aristolochic acid in the aetiology of endemic nephropathy-associated tumours. Int J Cancer. 2009;124:987–90.
8. Dracinska H, Barta F, Levova K, Hudecova A, Moserova M, Schmeiser HH, et al. Induction of cytochromes P450 1A1 and 1A2 suppresses formation of DNA adducts by carcinogenic aristolochic acid I in rats in vivo. Toxicology. 2016;344–346:7–18.
9. Schmeiser HH, Scherf HR, Wiessler M. Activating mutations at codon 61 of the c-Ha-ras gene in thin-tissue sections of tumors induced by aristolochic acid in rats and mice. Cancer Lett. 1991;59:139–43.
10. Stiborova M, Arlt VM, Schmeiser HH. DNA adducts formed by aristolochic acid are unique biomarkers of exposure and explain the initiation phase of upper urothelial cancer. Int J Mol Sci. 2017;18:2144.
11. Sborchia M, De Prez EG, Antoine MH, Bienfait L, Indra R, Valbuena G, et al. The impact of p53 on aristolochic acid I-induced nephrotoxicity and DNA damage in vivo and in vitro. Arch Toxicol. 2019;93:3345–66.
12. Bara T Jr., Gurzu S, Sugimura H, Bara T, Beleaua MA, Jung I. A systematic review of the possible carcinogenic role of the aristolochic acid. Rom J Morphol Embryol. 2017;58:41–4.
13. Chen CH, Dickman KG, Moriya M, Zavadil J, Sidorenko VS, Edwards KL, et al. Aristolochic acid-associated urothelial cancer in Taiwan. Proc Natl Acad Sci USA. 2012;109:8241–6.
14. Grollman AP. Aristolochic acid nephropathy: harbinger of a global iatrogenic disease. Environ Mol Mutagen. 2013;54:1–7.
15. Grollman AP, Shibutani S, Moriya M, Miller F, Wu L, Moll U, et al. Aristolochic acid and the etiology of endemic (Balkan) nephropathy. Proc Natl Acad Sci USA. 2007;104:12129–34.
16. Hoang ML, Chen CH, Chen PC, Roberts NJ, Dickman KG, Yun BH, et al. Aristolochic acid in the etiology of renal cell carcinoma. Cancer Epidemiol Biomark Prev. 2016;25:1600–8.
17. Lai MN, Wang SM, Chen PC, Chen YY, Wang JD. Population-based case-control study of Chinese herbal products containing aristolochic acid and urinary tract cancer risk. J Natl Cancer Inst. 2010;102:179–86.
18. Wang XM, Lu Y, Song YM, Dong J, Li RY, Wang GL, et al. Integrative genomic study of Chinese clear cell renal cell carcinoma reveals features associated with thrombus. Nat Commun. 2020;11:739.
19. Xiao Y, Ge M, Xue X, Wang C, Wang H, Wu X, et al. Hepatic cytochrome P450s metabolize aristolochic acid and reduce its kidney toxicity. Kidney Int. 2008;73:1231–9.
20. Xing GZ, Qi XM, Chen M, Wu YF, Yao J, Gong LK, et al. Comparison of the mutagenicity of aristolochic acid I and aristolochic acid II in the gpt delta transgenic mouse kidney. Mutat Res. 2012;743:52–8.
21. Xue X, Gong LK, Maeda K, Luan Y, Qi XM, Sugiyama Y, et al. Critical role of organic anion transporters 1 and 3 in kidney accumulation and toxicity of aristolochic acid I. Mol Pharmacol. 2011;8:2183–92.
22. Yang HY, Chen PC, Wang JD. Chinese herbs containing aristolochic acid associated with renal failure and urothelial carcinoma: a review from epidemiologic observations to causal inference. Biomed Res Int. 2014;2014:569325.
23. Pharmacopoeia Commission of the People's Republic of China. Pharmacopoeia of the People's Republic of China, vol 1. Beijing: China Medical Science Press; 2015.
24. Zhang HM, Zhao XH, Sun ZH, Li GC, Liu GC, Sun LR, et al. Recognition of the toxicity of aristolochic acid. J Clin Pharmacol Ther. 2019;44:157–62.
25. Ng AWT, Poon SL, Huang MN, Lim JQ, Boot A, Yu W, et al. Aristolochic acids and their derivatives are widely implicated in liver cancers in Taiwan and throughout Asia. Sci Transl Med. 2017;9:eaan6446.
26. Hawkins WE, Walker WW, Overstreet RM, Lytle JS, Lytle TF. Carcinogenic effects of some polycyclic aromatic hydrocarbons on the Japanese medaka and guppy in waterborne exposures. Sci Total Environ. 1990;94:155–67.
27. McCreery MQ, Halliwill KD, Chin D, Delrosario R, Hirst G, Vuong P, et al. Evolution of metastasis revealed by mutational landscapes of chemically induced skin cancers. Nat Med. 2015;21:1514–20.
28. Nassar D, Latil M, Boeckx B, Lambrechts D, Blanpain C. Genomic landscape of carcinogen-induced and genetically induced mouse skin squamous cell carcinoma. Nat Med. 2015;21:946–54.
29. Connor F, Rayner TF, Aitken SJ, Feig C, Lukk M, Santoyo-Lopez J, et al. Mutational landscape of a chemically-induced mouse model of liver cancer. J Hepatol. 2018;69:840–50.
30. Yu LX, Ling Y, Wang HY. Role of nonresolving inflammation in hepatocellular carcinoma development and progression. NPJ Precis Oncol. 2018;2:6. https://doi.org/10.1038/s41698-018-0048-z.
31. Zhu J, Yu H, Chen S, Yang P, Dong Z, Ling Y, et al. Prognostic significance of combining high mobility group Box-1 and OV-6 expression in hepatocellular carcinoma. Sci China Life Sci. 2018;61:912–23.
32. Arbuthnot P, Kew M. Hepatitis B virus and hepatocellular carcinoma. Int J Exp Pathol. 2001;82:77–100.
33. Bruix J, Reig M, Sherman M. Evidence-based diagnosis, staging, and treatment of patients with hepatocellular carcinoma. Gastroenterology. 2016;150:835–53.
34. Chen CJ, Yang YH, Lin MH, Lee CP, Tsan YT, Lai MN, et al. Herbal medicine containing aristolochic acid and the risk of hepatocellular carcinoma in patients with hepatitis B virus infection. Int J Cancer. 2018;143:1578–87.
35. Hong HH, Hoenerhoff MJ, Ton TV, Herbert RA, Kissling GE, Hooth MJ, et al. Kras, Egfr, and Tp53 mutations in B6C3F1/N mouse and F344/NTac rat alveolar/bronchiolar carcinomas resulting from chronic inhalation exposure to cobalt metal. Toxicol Pathol. 2015;43:872–82.
36. Yun BH, Xiao S, Yao L, Krishnamachari S, Rosenquist TA, Dickman KG, et al. A rapid throughput method to extract DNA from formalin-fixed paraffin-embedded tissues for biomonitoring carcinogenic DNA adducts. Chem Res Toxicol. 2017;30:2130–9.
37. Ito N, Tamano S, Shirai T. A medium-term rat liver bioassay for rapid in vivo detection of carcinogenic potential of chemicals. Cancer Sci. 2003;94:3–8.
38. Shirai T. A medium-term rat liver bioassay as a rapid in vivo test for carcinogenic potential: a historical review of model development and summary of results from 291 tests. Toxicol Pathol. 1997;25:453–60.
39. Tsuda H, Futakuchi M, Fukamachi K, Shirai T, Imaida K, Fukushima S, et al. A medium-term, rapid rat bioassay model for the detection of carcinogenic potential of chemicals. Toxicol Pathol. 2010;38:182–7.
40. Frazier KS, Seely JC, Hard GC, Betton G, Burnett R, Nakatsuji S, et al. Proliferative and nonproliferative lesions of the rat and mouse urinary system. Toxicol Pathol. 2012;40:14S–86S.

41. Thoolen B, Maronpot RR, Harada T, Nyska A, Rousseaux C, Nolte T, et al. Proliferative and nonproliferative lesions of the rat and mouse hepatobiliary system. Toxicol Pathol. 2010;38:5S–81S.
42. Nolte T, Brander-Weber P, Dangler C, Deschl U, Elwell MR, Greaves P, et al. Nonproliferative and proliferative lesions of the gastrointestinal tract, pancreas and salivary glands of the rat and mouse. J Toxicol Pathol. 2016;29:1S–125S.
43. Sato K, Kitahara A, Satoh K, Ishikawa T, Tatematsu M, Ito N. The placental form of glutathione S-transferase as a new marker protein for preneoplasia in rat chemical hepatocarcinogenesis. Gan. 1984;75:199–202.
44. Lu ZN, Luo Q, Zhao LN, Shi Y, Wang N, Wang L, et al. The mutational features of aristolochic acid-induced mouse and human liver cancers. Hepatology. 2020;71:929–42.
45. Hollstein M, Moriya M, Grollman AP, Olivier M. Analysis of TP53 mutation spectra reveals the fingerprint of the potent environmental carcinogen, aristolochic acid. Mutat Res. 2013;753:41–9.
46. McCreery MQ, Balmain A. Chemical carcinogenesis models of cancer: back to the future. Annu Rev Canc Biol. 2017;1:295–312.
47. Loeb LA, Harris CC. Advances in chemical carcinogenesis: a historical review and prospective. Cancer Res. 2008;68:6863–72.
48. Groos J, Bannasch P, Schwarz M, Kopp-Schneider A. Comparison of mode of action of four hepatocarcinogens: a model-based approach. Toxicol Sci. 2007;99:446–54.
49. Demetriou CA, Degli Esposti D, Pullen Fedinick K, Russo F, Robinson O, Vineis P. Filling the gap between chemical carcinogenesis and the hallmarks of cancer: a temporal perspective. Eur J Clin Invest. 2018;48:e12933.
50. Hanahan D, Weinberg RA. Hallmarks of cancer: the next generation. Cell. 2011;144:646–74.
51. International Council for Harmonisation. S1B: Testing for carcinogenicity of pharmaceuticals. Geneva, Switzerland: ICH; 1998.
52. Poon SL, Huang MN, Choo Y, McPherson JR, Yu W, Heng HL, et al. Mutation signatures implicate aristolochic acid in bladder cancer development. Genome Med. 2015;7:38.
53. National Toxicology Program. Final report on carcinogens background document for aristolochic acids. Rep Carcinog Backgr Doc. 2008;i–xxv:1–246.
54. Dickman KG, Sweet DH, Bonala R, Ray T, Wu A. Physiological and molecular characterization of aristolochic acid transport by the kidney. J Pharmacol Exp Ther. 2011;338:588–97.
55. Stiborova M, Frei E, Schmeiser HH. Biotransformation enzymes in development of renal injury and urothelial cancer caused by aristolochic acid. Kidney Int. 2008;73:1209–11.
56. Uno Y, Takata R, Kito G, Yamazaki H, Nakagawa K, Nakamura Y, et al. Sex- and age-dependent gene expression in human liver: An implication for drug-metabolizing enzymes. Drug Metab Pharmacokinet. 2017;32:100–7.
57. Stiborova M, Barta F, Levova K, Hodek P, Schmeiser HH, Arlt VM, et al. A mechanism of o-demethylation of aristolochic acid i by cytochromes p450 and their contributions to this reaction in human and rat livers: experimental and theoretical approaches. Int J Mol Sci. 2015;16:27561–75.
58. Rosenquist TA, Einolf HJ, Dickman KG, Wang L, Smith A, Grollman AP. Cytochrome P450 1A2 detoxicates aristolochic acid in the mouse. Drug Metab Dispos. 2010;38:761–8.
59. Stiborova M, Frei E, Arlt VM, Schmeiser HH. The role of biotransformation enzymes in the development of renal injury and urothelial cancer caused by aristolochic acid: urgent questions and difficult answers. Biomed Pap Med Fac Univ Palacky Olomouc Czech Repub. 2009;153:5–11.
60. Stiborova M, Levova K, Barta F, Shi Z, Frei E, Schmeiser HH, et al. Bioactivation versus detoxication of the urothelial carcinogen aristolochic acid I by human cytochrome P450 1A1 and 1A2. Toxicol Sci. 2012;125:345–58.
61. Li HS, Ji HN, Song NN, Li B, Sui F, Li YF, et al. Study on the difference of liver metabolism spectrum among different species, sexes and ages of mice. Chin J Pharmacov. 2020;17:6–16.
62. Mengs U, Lang W, Poch JA. The carcinogenic action of aristolochic acid in rats. Arch Toxicol. 1982;51:107–19.
63. Mengs U. Tumour induction in mice following exposure to aristolochic acid. Arch Toxicol. 1988;61:504–5.
64. Matsushita K, Kuroda K, Ishii Y, Takasu S, Kijima A, Kawaguchi H, et al. Improvement and validation of a medium-term gpt delta rat model for predicting chemical carcinogenicity and underlying mode of action. Exp Toxicol Pathol. 2014;66:313–21.
65. Denda A, Kitayama W, Konishi Y, Yan Y, Fukamachi Y, Miura M, et al. Genetic properties for the suppression of development of putative preneoplastic glutathione S-transferase placental form-positive foci in the liver of carcinogen-resistant DRH strain rats. Cancer Lett. 1999;140:59–67.
66. Higashi K, Hiai H, Higashi T, Muramatsu M. Regulatory mechanism of glutathione S-transferase P-form during chemical hepatocarcinogenesis: old wine in a new bottle. Cancer Lett. 2004;209:155–63.
67. Zeng ZZ, Higashi S, Kitayama W, Denda A, Yan Y, Matsuo K, et al. Genetic resistance to chemical carcinogen-induced preneoplastic hepatic lesions in DRH strain rats. Cancer Res. 2000;60:2876–81.
68. Li R, Du Y, Chen Z, Xu D, Lin T, Jin S, et al. Macroscopic somatic clonal expansion in morphologically normal human urothelium. Science. 2020;370:82–9.
69. Martinek V, Barta F, Hodek P, Frei E, Schmeiser HH, Arlt VM, et al. Comparison of the oxidation of carcinogenic aristolochic acid I and II by microsomal cytochromes P450 in vitro: experimental and theoretical approaches. Monatsh Chem. 2017;148:1971–81.
70. Chen M, Gong L, Qi X, Xing G, Luan Y, Wu Y, et al. Inhibition of renal NQO1 activity by dicoumarol suppresses nitroreduction of aristolochic acid I and attenuates its nephrotoxicity. Toxicol Sci. 2011;122:288–96.
71. Levova K, Moserova M, Nebert DW, Phillips DH, Frei E, Schmeiser HH, et al. NAD(P)H:quinone oxidoreductase expression in Cyp1a-knockout and CYP1A-humanized mouse lines and its effect on bioactivation of the carcinogen aristolochic acid I. Toxicol Appl Pharmacol. 2012;265:360–7.
72. Stiborova M, Fernando RC, Schmeiser HH, Frei E, Pfau W, Wiessler M. Characterization of DNA adducts formed by aristolochic acids in the target organ (forestomach) of rats by ^{32}P-postlabelling analysis using different chromatographic procedures. Carcinogenesis. 1994;15:1187–92.
73. Bieler CA, Stiborova M, Wiessler M, Cosyns JP, van Ypersele de Strihou C, Schmeiser HH. ^{32}P-post-labelling analysis of DNA adducts formed by aristolochic acid in tissues from patients with Chinese herbs nephropathy. Carcinogenesis. 1997;18:1063–7.
74. Stiborova M, Frei E, Breuer A, Bieler CA, Schmeiser HH. Aristolactam I a metabolite of aristolochic acid I upon activation forms an adduct found in DNA of patients with Chinese herbs nephropathy. Exp Toxicol Pathol. 1999;51:421–7.
75. Baudoux TE, Pozdzik AA, Arlt VM, De Prez EG, Antoine MH, Quellard N, et al. Probenecid prevents acute tubular necrosis in a mouse model of aristolochic acid nephropathy. Kidney Int. 2012;82:1105–13.
76. Bakhiya N, Arlt VM, Bahn A, Burckhardt G, Phillips DH, Glatt H. Molecular evidence for an involvement of organic anion transporters (OATs) in aristolochic acid nephropathy. Toxicology. 2009;264:74–9.
77. Chang SY, Weber EJ, Sidorenko VS, Chapron A, Yeung CK, Gao C, et al. Human liver-kidney model elucidates the mechanisms of aristolochic acid nephrotoxicity. JCI Insight. 2017;2:e95978.
78. Han J, Xian Z, Zhang Y, Liu J, Liang A. Systematic overview of aristolochic acids: nephrotoxicity, carcinogenicity, and underlying mechanisms. Front Pharmacol. 2019;10:648.
79. Yun BH, Rosenquist TA, Sidorenko V, Iden CR, Chen CH, Pu YS, et al. Biomonitoring of aristolactam-DNA adducts in human tissues using ultra-performance liquid chromatography/ion-trap mass spectrometry. Chem Res Toxicol. 2012;25:1119–31.
80. Hayashi Y. Overview of genotoxic carcinogens and non-genotoxic carcinogens. Exp Toxicol Pathol. 1992;44:465–71.
81. Nohmi T. Thresholds of genotoxic and non-genotoxic carcinogens. Toxicol Res. 2018;34:281–90.
82. Pharmacopoeia commission of the People's Republic of China. Pharmacopoeia of the People's Republic of China, vol 1. Beijing: China Medical Science Press; 2020.